NUMERICAL STUDY ON COHERENT HARMONIC GENERATION FREE ELECTRON LASER SEEDED BY CHIRPED EXTERNAL LASER*

H. Zen, M. Adachi, M. Katoh, UVSOR, Okazaki, Japan
T. Tanikawa, SOKENDAI, Okazaki, Japan
Y. Taira, N. Yamamoto, M. Hosaka, Nagoya University, Nagoya, Japan

Abstract

A numerical simulation code which can take the effect of seed laser chirping on Coherent Harmonic Generation Free Electron Laser (CHG-FEL) into account has been developed. By the code, an impressive previous result of CHG-FEL, whose spectrum having intense sidebands, was well reproduced. The code predicted that the temporal distribution of 3rd harmonic component of CHG-FEL has three peaks in one pulse. The developed code will contribute to deeper understanding of CHG-FEL.

INTRODUCTION

CHG-FEL is one of the promising ways to generate coherent and short pulse VUV radiations. Recently, many successful experimental results [1-5] have been reported. One impressive result on named synchrotron sideband was obtained at UVSOR and reported in ref [1]. In the paper, numerical analysis on the sidebands was also reported and the analysis qualitatively succeeded in reproducing the experimental results at saturation regime of CHG-FEL. However, there were large discrepancies in spectral shape between the experimental and numerical results. The separation and width of measured sidebands are ten times larger than the numerical result.

We considered that the large discrepancy was caused by difference of frequency chirp property of seed laser in the experiment and for the analysis. The seed laser was chirped in the experiment and was treated as a transform limited pulse in the analysis. To correctly analyze the sideband phenomena of CHG-FEL, we developed a numerical calculation code which can take the effect of seed laser chirping into account.

In next section, detail of the developed code is described. The parameters for calculation are shown in subsequent section. And the following section is devoted to calculation results. In the section, at first, typical calculation results are presented. Next, the calculation results are compared with experimental results reported in ref [1]. In last subsection, the temporal distribution of CHG-FEL pulse in the previous experiment was predicted from the result of developed code.

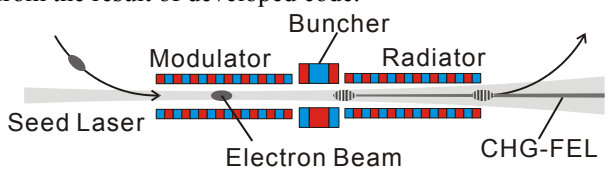

Figure 1 : Schematic layout of CHG-FEL.

*zen@ims.ac.jp

CALCULATION METHOD

Figure 1 shows a schematic drawing of CHG-FEL. A seed laser and an electron bunch are coaxially injected to the optical klystron. Through the interaction between the laser and the electron bunch, harmonic radiations are emitted from the bunch.

We made particle-by-particle calculation for simulating the CHG-FEL. As the initial electron distribution at the entrance of modulator, a huge number of macro-particles having uniform temporal distribution and Gaussian energy distribution are generated. For each particle, interaction with the seed laser in the modulator is solved and energy dependent phase shift in the buncher is added. For the radiator, interference of emitted fields in the radiator is only taken into account. In the following subsections, detailed calculation methods are described.

Modulator

To simulate the FEL interaction in the modulator, the dimensionless 1D FEL equations are used in this study under slowly varying envelope approximation [6]. In storage ring CHG-FEL, length of the modulator is short and peak current of electron beam is not so high. Therefore, amplification of optical field in the modulator is negligible and neglected in this study to simplify the calculation. The solved equations are followings,

$$\frac{d\Psi_j(\tau)}{d\tau} = \mu_j(\tau) \ , \tag{1}$$

$$\frac{d\mu_j(\tau)}{d\tau} = \mathrm{Re}\left[ia(\zeta,\tau)\exp\{i\Psi_j(\tau)\}\right] , \tag{2}$$

where $\Psi_j(\tau)=(k_w+k_L)z_j(t)-\omega_L t$ is the electron phase, $\mu_j(\tau)=4\pi N_M[\gamma_j-\gamma_r]/\gamma_r$ is the dimensionless electron energy, $\tau=ct/N_M\lambda_w$ is the dimensionless time, $\zeta_j=[z_j(\tau)-N_M\lambda_w\tau]/\lambda_L$ is the longitudinal position of jth electron and $a(\zeta,\tau)$ is the dimensionless field envelope, which is defined by

$$a(\zeta,\tau) = \frac{4\pi e a_w \lambda_w [J_0(\xi)-J_1(\xi)]N_M^2}{\gamma_r^2 m_0 c^2} E(\zeta,\tau)e^{i\phi_L(\zeta,\tau)} . \tag{3}$$

Here a_w is undulator parameter, $\lambda_L=2\pi/k_L$ is the seed laser wavelength, $\lambda_w=2\pi/k_w$ is the period length of modulator, $\gamma_r=[(\lambda_w/\lambda_L)(1+a_w^2)/2]^{1/2}$ is the resonant energy, N_M is the period number of modulator, $E(\zeta,\tau)$ is the rms optical field strength and $\phi_L(\zeta,\tau)$ is the laser phase.

Buncher

In a buncher section, electron beam does not change its energy and only the phase of the electron changes as given by following equation [7],

$$\Delta\Psi_j = \frac{N_\mathrm{d}}{N_\mathrm{M}}\mu_j - 2\pi N_\mathrm{d} \ , \tag{4}$$

where N_d indicates the number of equivalent periods in dispersive section, which dominates the bunching property of the buncher.

After the buncher, we obtain phase (temporal) distribution of the electron beam as an array I_n by calculating

$$I_n = \sum_{j=0}^{N} H(\Psi_j, \Psi_n, \delta\Psi/2)$$
$$H(a,b,c) = \begin{cases} 1 & if\ (b-c) < a < (b+c) \\ 0 & if\ a < (b-c) \bigcap (b+c) < a \end{cases} \tag{5}$$

where Ψ_n is the central phase of nth element of the array and $\delta\Psi$ is the width of each element. To obtain kth harmonic component, $\delta\Psi$ should be smaller than π/k for frequency analysis.

Radiator

In radiator, interaction between the electron beam and optical fields is neglected for simplicity. And only interference of radiation field is taken into account. As shown in Fig. 2, we assume that the electric field is only emitted at the each peak of sinusoidal electron trajectory. In practical calculation, the final electric field is given by

$$E_{n,\mathrm{norm}} = \sum_{m=1}^{2N_\mathrm{R}} (-1)^{m-1} I_{n+m\delta\Psi/2} \ , \tag{6}$$

where $E_{n,\mathrm{norm}}$ is the radiated field normalized by single electron field and N_R is the period number of the radiator.

As the result of whole calculation, we obtain temporal evolution of radiation electric field, which contains all harmonic components. And by using a Fast Fourier Transform (FFT) code supplied in Origin [8], frequency and wavelength spectrum are obtained.

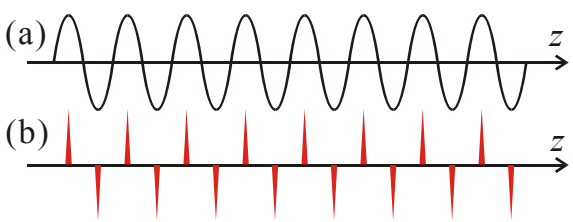

Figure 2: Schematic drawing of calculation in radiator. (a) Electron trajectory in radiator, (b) assumed electric field emitted from single electron in radiator.

Treatment for Chirped Laser

In this study, we focused on the effect of seed laser chirping on CHG-FEL. We tried to introduce the chirping effect into 1D-FEL calculation.

We assumed paraxial Gaussian temporal distribution of the laser. Then the electric field of the chirped laser can be described in the formula,

$$E(t,z) = E_0 \exp[-(b_1 + ib_2)(z-ct)^2]\exp[\mathrm{i}(k_\mathrm{L} z - \omega_\mathrm{L} t)], \tag{7}$$

$$b_1 = \frac{2\ln 2}{c^2\Delta\tau_\mathrm{L}^2}, \ b_2^2 = \frac{\Delta\omega^2}{4c^2\Delta\tau_\mathrm{L}^2} - \left(\frac{2\ln 2}{c^2\Delta\tau_\mathrm{L}^2}\right)^2, \tag{8}$$

where E_0 is the peak electric field, $\Delta\tau_\mathrm{L}$ is FWHM pulse duration and $\Delta\omega \approx 2\pi c\Delta\lambda/\lambda_\mathrm{L}^2$ is the FWHM bandwidth of the laser. When b_2 equals to zero, $\Delta\omega\Delta\tau_\mathrm{L} = 8\ln 2 \times \sigma_\omega\sigma_\tau = 4\ln 2$ is satisfied and this means that the pulse is Transform Limited (TL) pulse ($\sigma_\omega\sigma_\tau = 1/2$). From Eq. (7), the field envelope $E(\zeta,\tau)$ in Eq. (3) and the laser phase $\phi_\mathrm{L}(\zeta,\tau)$ are determined as $E_0\exp[-b_1(\lambda_\mathrm{L}\zeta)^2]$ and $-b_2(\lambda_\mathrm{L}\zeta)^2$, respectively.

For example, the field envelope of 1-ps TL pulse and 1-ps chirped pulse with $\Delta\lambda_\mathrm{L}$=7 nm are plotted in Fig. 3. In the case of TL pulse (Fig. 3 (a)), the imaginary part of the field envelope is constant and zero. On the other hand, for chirped pulse, the real and imaginary parts of the field envelope have large oscillation due to quadratic shift of the phase.

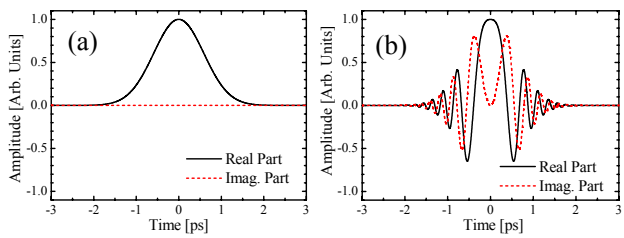

Fig. 3: Example of field envelope. (a) 1-ps TL pulse, (b) 1-ps chirped pulse with 7 nm bandwidth.

Table 1 : Parameters for calculation

Electron Beam	
Energy	600 MeV
Energy Spread (RMS)	3.4×10^{-4}
Optical Klystron	
Period Length	110 mm
Number of Period	9 (modulator) 9 (radiator)
Equivalent Period Number in Buncher N_d	45
Undulator Parameter a_w	4.37
Seed Laser	
Central Wavelength	800 nm

CALCULATION PARAMETERS

The parameters for calculation are listed in Table 1, which is almost same with experimental parameter for CHG-FEL in UVSOR.

In the calculations, 4×10^7 macro-particles, which have 5-ps uniform temporal distribution and Gaussian energy distribution with RMS energy spread of 3.4×10^{-4} were used as initial distribution at the entrance of the modulator. And $\delta\Psi$ was selected as $\pi/10$.

RESULTS

Typical Result Obtained by Developed Code

A typical calculation result is shown in Fig. 4, which was calculated under the seed laser condition of $\Delta\tau_L$=1 ps-FWHM, $\Delta\lambda_L$= 7 nm and E_0=101 MV/m. As aforementioned in the previous section, the electric field of CHG-FEL is given by the developed code as shown in Fig. 4 (a) and (b). From the electric field, frequency (or wavelength) spectrum of the CHG-FEL can be obtained by FFT analysis. The results are shown in Fig. 4 (c) and (d). Because the calculation started from random distribution and included the interference of radiation field at the radiator, spontaneous radiation from the radiator was naturally included in this calculation (black lines in (c) and (d)).

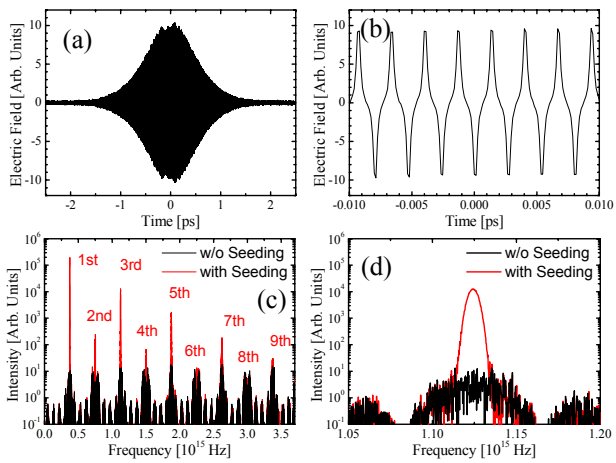

Figure 4: Typical results of the developed code. (a) CHG-FEL electric field, (b) magnified plot of (a), (c) frequency spectrum of (a), and (d) magnified plot of (c) around the 3rd harmonics.

Comparison with Previous Experiment

Figure 5 shows the results of the previous experiments [1]. As shown in Fig. 5 (d), sidebands of CHG-FEL were observed when it is seeded by strong focusing laser. The separation of the sidebands was around 3 nm and the width of each peak was around 1 nm. In ref [1] Fig. 3 (b)-(v), the sideband separation was just 0.3 nm and width was 0.1 nm, which are ten times narrower than the experimental result.

We carried out numerical simulation with TL pulse and chirped pulse, and compared those spectra with the reported ones. Figure 6 shows results of the simulation. The sideband separation and peak width of calculated spectra with TL pulse (Fig. 6 (a)) agreed well with numerical results reported in ref [1]. On the contrary, the spectra with the chirped seed laser (Fig. 6 (b)) shows quite similar shape with experimental result. The sidebands separation (3 nm) and width (1 nm) agreed well with those of previous experiment. This agreement validates adequacy of our code and its algorithm.

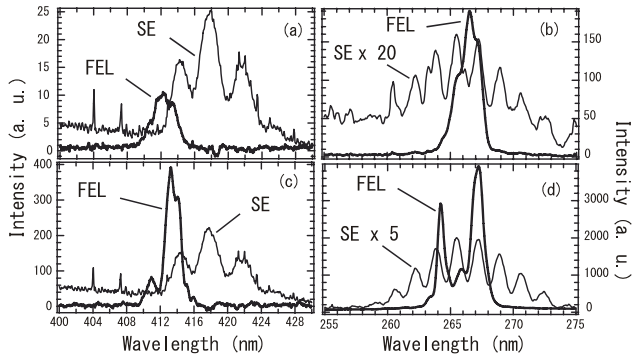

Figure 5: CHG-FEL spectra results previously measured at UVSOR and reported in ref. [1]. (a) Second and (b) third harmonics with smooth focusing seed laser, (c) second and (b) third harmonics with strong focusing seed laser. The laser pulse energy and pulse duration were 2 mJ and 1 ps-FWHM, respectively.

As discussed in ref [1], the origin of the sideband is over-bunching of electron micro-bunch. However, in the case of chirped seeding, seed laser field has large phase shift itself. The laser originated phase shift is much larger than the phase shift induced by the synchrotron oscillation of electron which has been discussed in ref [1]. Therefore, neglecting the chirping effect leaded to the large discrepancies between the experiment and simulation in ref [1]. These results indicated that the chirping effect should be taken into account for discussing the spectral property of CHG-FEL.

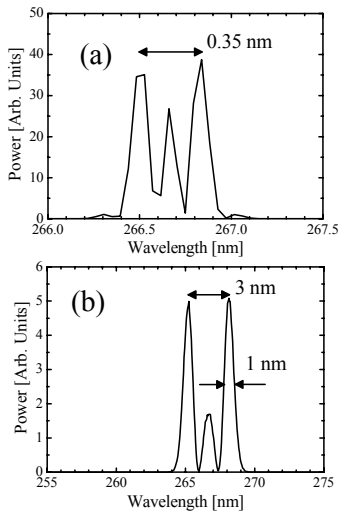

Figure 6: Calculation results of the developed code. (a) $\Delta\tau_L$=1 ps-FWHM, TL pulse and E_0 = 914 MV/m, (b) $\Delta\tau_L$=1 ps-FWHM, $\Delta\lambda_L$=7 nm and E_0 = 914 MV/m.

Prediction of Temporal Evolution of CHG-FEL Pulse Having Reported Spectrum

In last subsection, the calculation result with chirped laser (Fig. 6 (b)) showed good agreement with previous experimental result (Fig. 5 (d)). As aforementioned, our code can give temporal evolution of electric field of CHG-FEL radiation. In this subsection, temporal distribution of the numerical result is discussed.

The 3rd harmonic component of CHG-FEL under the same condition with Fig. 6 was extracted from the calculated electric field by applying frequency filter to the field. The power evolution of 3rd harmonics is shown in Fig. 7. When the spectral distribution shown in Fig. 6 (b) is observed, the temporal distribution of 3rd harmonic radiation probably has three peaks in one pulse as shown in Fig. 7.

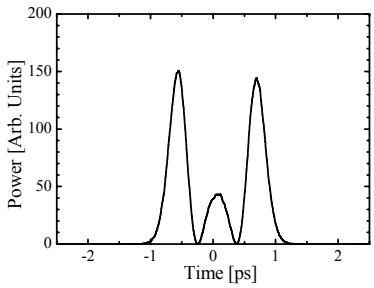

Figure 7: Predicted temporal evolution of 3rd harmonic CHG-FEL power under the same condition with Fig. 6.

CONCLUSION

A numerical simulation code which can take the seed laser chirping into account has been developed. The previous experimental result, which observed sidebands in its spectrum, was quantitatively well reproduced by the code. In addition, validity of the code was proven. Moreover, the temporal distribution was predicted to have three peaks in one pulse.

The developed code will contribute to deeper understanding of CHG-FEL property and seeded FEL.

REFERENCES

[1] M. Labat et al., Phys. Rev. Lett. **102**, 014801 (2009).
[2] M. Labat et al., Eur. Phys. J. D **44**, 187–200 (2007).
[3] G. De Ninno et al., Phys. Rev. Lett. **101**, 053902 (2008).
[4] M. Labat et al., Phys. Rev. Lett. **101**, 164803 (2008).
[5] T. Tanikawa et al., Proc. of IPAC10, pp.2206-2208 (2010).
[6] C.A. Brau, Free-Electron Lasers, Academic Press Inc. pp. 87-89 (1990).
[7] Q. Jia, PR-ST AB, **8**, 060701 (2005).
[8] OriginLab, http://www.originlab.com/